Analytical solution for estimating surface settlements induced by multiple tunnel excavation

ZHOU Xiao-wen[1], NG C W W[2]

(1. South China University of Technology, Guangzhou 510640, China; 2. Hong Kong University of Science and Technology, Hong Kong)

Abstract: The derivation of an approximate explicit analytical solution was presented to calculate three-dimensional surface settlements due to the excavation of either single or multiple tunnels in a homogeneous elastic soil. This solution was based on the integrated form of Mindlin's equations and Taylor's series expansions. Surface settlements due to the construction of tunnels with an arbitrary orientation during the tunnel advancement with and without supporting pressure could be modelled by using a stress relief coefficient. The derived analytical solution was verified by carrying out a three-dimensional finite element analysis of a single tunnel excavation. The discrepancy between the simplified approximate solution and the finite element analysis was less than 9%. The usefulness of the simplified approximate analytical solution was demonstrated by analyzing two parallel and two cross tunnels.

Key words: analytical solution; multiple tunnels; settlement; Mindlin's equation

CLC number: U452 **Document code:** A **Article ID:** 1000 - 4548(2007)11 - 1703 - 08

Biography: ZHOU Xiao-wen (1965 -), male, Professor. His interest is the properties of soils and the safety evaluation of soil structures. E-mail: xwzhou126@126.com.

用于估计多隧道开挖地面沉降的解析解

周小文[1]，吴宏伟[2]

(1. 华南理工大学，广东 广州 510640；2. 香港科技大学，香港)

摘 要：对于均质弹性地基中单隧道和多隧道开挖施工，本文给出了用于计算二维和三维地面沉降的近似的显式解析解。该解析解是对点荷载下 Mindlin 位移解进行积分并利用泰勒级数展开而得。利用该解析解，可以计算多个任意相对位置的隧道掘进引起的地面沉降。对于隧道开挖面不同支护程度的情况，可以采用一个原位应力释放度（系数）来模拟。通过一个单隧道开挖的弹性有限元计算对比，对简化的解析解进行了检验，两者计算结果的差距在 9%以内。简化解析解的有效性，通过两种情况（两条相互平行隧道和两条相互垂直隧道）的计算得到验证。

关键词：解析解；多隧道；沉降；明德林方程

0 Introduction

Prediction of surface ground movements due to tunnelling in urban areas is essential. Two different approaches may be identified for the prediction, namely, empirical methods and theoretical approaches including analytical and numerical methods. Peck[1] and many others such as O'Reilly and New[2], Attewell and Woodman [3] proposed the use of a Gaussian distribution to approximate the transverse and the longitudinal surface settlement trough over a tunnel, respectively. Despite of the great success of the empirical methods for engineering applications, these methods do not contribute to scientific advancement significantly and have severe limitations on the prediction of three-dimensional ground settlements. The use of the numerical methods such as the finite element method can potentially overcome some of the shortcomings of the empirical methods. However, the benefits of using the numerical methods are often outweighed by the sophistication of constitutive models and parameters involved and the high demand of modelling techniques required.

Sagaseta[4] presented a closed form analytical solution for the strain field in an initially isotropic and homogeneous incompressible soil due to near-surface ground loss. His results are simple, especially for the

Received date: 2006 - 10 - 12

movements of soil surface in an undrained manner. Sagaseta's solution is very useful for cases in which the imposed boundary conditions are only or mainly in terms of displacements, i.e., strain-controlled problems such as the use of volume loss to estimate ground settlements. Verruijt and Booker[5] generalized Sagaseta's solution for both incompressible and compressible cases and included the effect of tunnel ovalization. The accuracy of these methods depends on the appropriateness of an estimated ground loss. However, three important limitations of the developed analytical solutions such as the prediction of three-dimensional ground settlement profiles, the effects of multiple parallel or cross tunnels interaction and the influence of supporting pressure variation on ground settlements cannot be overcome easily. In this paper, a simple approximate analytical solution based on the Mindlin's equations[6] is derived to overcome the three limitations. The derived analytical solution is verified by carrying out a three-dimensional finite element analysis.

1 The approximate analytical solution

The solution consists of two parts: shift of the origin of the Mindlin's equations for calculating displacements due to point forces and making use of the equations to obtain settlements at the ground surface due to stress changes associated with an excavation of an arbitrary cylindrical volume of soil.

1.1 Shift of origin for Mindlin's equations

Mindlin's original equations were set up in a coordinate system in which point forces are applied along z-axis at $(0,\ 0, w)$. In the case of point forces acting at an arbitrary point (u,v,w), shift of the origin is required for using the Mindlin's equations (Vaziri, et al[7]). As shown in Figure 1, three point forces, P, Q and T are applied at a point (u,v,w), respectively at the positive z-, x- and y-axis. For any point (x,y,z) within the half-space, the displacements induced by the three point forces can be derived by coordinate shift in Mindlin's original equations. Just vertical displacement (i.e., settlement) at the ground surface is concerned in this paper. Thus at any point $(x,y,0)$ the following formulas are obtained by the shift of origin:

$$\delta_P = \frac{P}{4\pi G}\left[\frac{2(1-\mu)}{R}+\frac{w^2}{R^3}\right] \quad , \qquad (1a)$$

$$\delta_Q = \frac{Q(x-u)}{4\pi G}\left[\frac{-w}{R^3}+\frac{(1-2\mu)}{R(R+w)}\right] \quad , \qquad (1b)$$

$$\delta_T = \frac{T(y-v)}{4\pi G}\left[\frac{-w}{R^3}+\frac{(1-2\mu)}{R(R+w)}\right] \quad . \qquad (1c)$$

where δ_P, δ_Q and δ_T are the vertical displacements induced by the point forces P, Q and T, respectively; G is the shear modulus and μ is the Poisson's ratio of the elastic soil; $R=\sqrt{(x-u)^2+(y-v)^2+w^2}$.

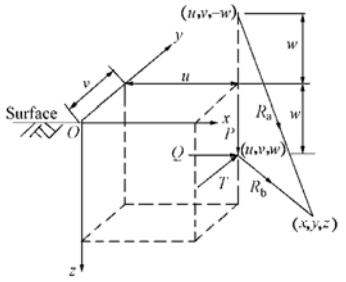

Fig. 1 Coordinate system

It should be noted that the point forces P, Q and T can be simply replaced by force increments, ΔP, ΔQ and ΔT, if one is only interested in vertical displacement due to stress changes in the ground, for instance, the stress change in tunnelling advance.

1.2 Configuration of tunnel excavation and stress changes

Figure 2 shows the geometry of a horizontal circular tunnel to be excavated. The longitudinal centre line of the tunnel, parallel to the y-axis, is located at a depth, h, below the ground surface. The circular tunnel with radius r_0 starts at $y=v_1$ and ends at $y=v_2$, i.e., an arbitrary length L of the tunnel is equal to v_2-v_1. For calculating surface settlement at any point $(x,y,0)$ due to stress (or force) changes as a result of the tunnel excavation, changes of forces acting on three boundary excavation surfaces of the tunnel should be considered, i.e., two end cross-sections symbolised by EF_1 and EF_2, and the cylindrical curved surface (CF).

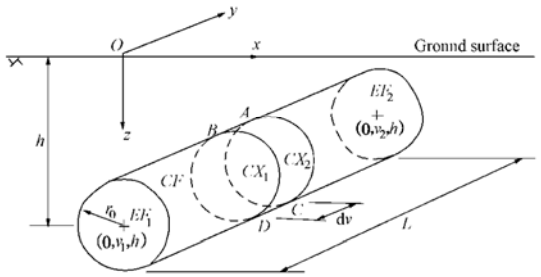

Fig. 2 Geometry of tunnel

To calculate the induced settlement, one can consider the excavation of an infinitesimal thin slice *ABCD* with thickness (or length) dv of the tunnel shown in Figure 2 first. This infinitesimal thin cylindrical slice is bounded by two vertical faces, CX_1 and CX_2. Therefore, the total induced settlement is the sum of the contribution from each infinitesimal thin slice, the sum can be obtained by integration to v.

1.3 Surface settlement induced by excavation of an infinitesimal thin slice

Figure 3(a) shows an arbitrary curved surface 1234 located on the infinitesimal thin slice *ABCD*. The changes of forces, dP and dQ, acting on the surface in the respective x- and z-direction as a result of tunnel excavation are shown in Figure 3(b).

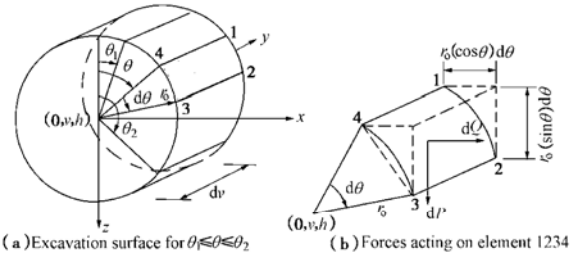

Fig. 3 Forces acting on curved surface *ABCD*

To determine the magnitudes of dP and dQ, it is assumed that the initial horizontal effective stress in the ground can be calculated from the earth pressure coefficient at rest, k_0. To facilitate possible modelling of a pressurized tunnel during construction, a positive stress relief parameter, k, is introduced and defined as follows:

$$k = \Delta\sigma_{\mathrm{v}} / \sigma_{\mathrm{v0}} \quad , \tag{2}$$

where σ_{v0} is the initial effective overburden pressure, $\Delta\sigma_{\mathrm{v}}$ is an effective stress reduction (relief) in vertical direction. If k =1, this means that no supporting pressure is applied inside the tunnel (i.e., full release of stress). On the other hand, if 0< k <1, this means that some supporting pressure is provided inside the tunnel during excavation (partial stress relief). Of course, if k =0, no change of stress (no relief) is permitted or imposed.

With the above considerations and reference to Figure 3, the changes of forces dP and dQ due to tunnelling can be readily written as follows:

$$\mathrm{d}P = k\sigma_{v0}(A_{1234}\cos\theta) = k\rho h r_0 \cos\theta \mathrm{d}\theta \mathrm{d}v \ , \tag{3a}$$

$$\mathrm{d}Q = -kk_0\sigma_{v0}(A_{1234}\sin\theta)\mathrm{d}\theta\mathrm{d}v = -kk_0\rho h r_0 \sin\theta \mathrm{d}\theta\mathrm{d}v \ , \tag{3b}$$

where ρ is the density of the ground, σ_{v0} (= ρh) is the initial overburden earth pressure acting at the depth of tunnel center, θ is the clockwise angle measuring from the crown of tunnel, A_{1234} (= $r_0\mathrm{d}\theta\mathrm{d}v$) is the area of the infinitesimal small curved element 1234, $r_0\cos\theta\mathrm{d}\theta\mathrm{d}v$ and $r_0\sin\theta\mathrm{d}\theta\mathrm{d}v$ are its projections on the horizontal and vertical planes respectively (see Figure 3(b)).

For the two boundary faces CX_1 and CX_2 (see Figure 2), the horizontal force change $\mathrm{d}T_1$ acting on an infinitesimal fan-shaped area 1′2′3′4′ (i.e., $A_{1'2'3'4'}$ (= $r\mathrm{d}\theta\mathrm{d}r$)) along the longitudinal direction (y-axis) of the tunnel (see Figure 4) during excavation can be written as follows:

$$\mathrm{d}T_1 = kk_0\sigma_{v0}A_{1'2'3'4'} = kk_0\rho h r \mathrm{d}\theta\mathrm{d}r \ . \tag{3c}$$

where r is the radial distance of the element from the centre of the tunnel, $0 \le r \le r_0$.

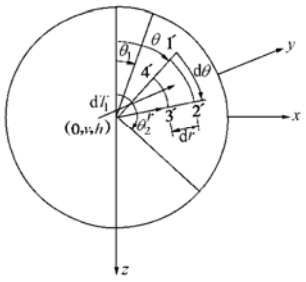

Fig. 4 Forces acting on cross-section

For the opposite cross-section CX_2, the corresponding force change $\mathrm{d}T_2$ is:

$$\mathrm{d}T_2 = -\mathrm{d}T_1 = -kk_0\rho h r \mathrm{d}\theta\mathrm{d}r \tag{3d}$$

The point forces dP and dQ are both acting at $(r_0\sin\theta, v, h - r_0\cos\theta)$, whereas $\mathrm{d}T_1$ and $\mathrm{d}T_2$ are locating at $(-r\sin\theta, v_1, h - r\cos\theta)$ and $(-r\sin\theta, v_2$, $h - r\cos\theta)$, respectively.

For any surface point ($x, y, 0$), the settlement components, $\delta_{\mathrm{d}P}, \delta_{\mathrm{d}Q}, \delta_{\mathrm{d}T_1}$ and $\delta_{\mathrm{d}T_2}$ can be obtained by substituting Equations 3(a)~(d) into Equations 1(a)~(c) as follows:

$$\delta_{\mathrm{d}P} = k\frac{(1-\mu)\rho h r_0}{2\pi G}\frac{\cos\theta}{R_{CF}}\mathrm{d}\theta\mathrm{d}v + k\frac{\rho h r_0}{4\pi G}\frac{\cos\theta(h - r_0\cos\theta)^2}{R_{CF}^3}\mathrm{d}\theta\mathrm{d}v \ , \tag{4a}$$

$$\delta_{\mathrm{d}Q} = kk_{\mathrm{o}}\frac{\rho h r_0}{4\pi G}\frac{\sin\theta(x - r_0\sin\theta)(h - r_0\cos\theta)}{R_{CF}^3}\mathrm{d}\theta\mathrm{d}v - kk_0\frac{\rho(1-2\mu)h r_0}{4\pi G}\frac{\sin\theta(x - r_0\sin\theta)}{R_{CF}(R_{CF} + h - r_0\cos\theta)}\mathrm{d}\theta\mathrm{d}v \ , \tag{4b}$$

$$\delta_{dT_1} = -kk_o \frac{\rho h(y-v)}{4\pi G} \frac{r(h-r\cos\theta)}{R_{CX}^3} \mathrm{d}r\mathrm{d}\theta +$$
$$kk_0 \frac{\rho h(1-2\mu)(y-v)}{4\mathrm{p}G} \frac{r}{R_{CX}(R_{CX}+h-r\cos\theta)} \mathrm{d}r\,\mathrm{d}\theta \text{ , (4c)}$$

$$\delta_{dT_2} = kk_0 \frac{\rho h(y-v)}{4\pi G} \frac{r(h-r\cos\theta)}{R_{CX}^3} \mathrm{d}r\mathrm{d}\theta -$$
$$kk_0 \frac{\rho h(1-2\mu)(y-v)}{4\pi G} \frac{r}{R_{CX}(R_{CX}+h-r\cos\theta)} \mathrm{d}r\mathrm{d}\theta \text{ , (4d)}$$

where

$$R_{CF} = \sqrt{(x-r_0\sin\theta)^2+(y-v)^2+(h-r_0\cos\theta)^2} \text{ ,}$$
$$R_{CX} = \sqrt{(x-r\sin\theta)^2+(y-v)^2+(h-r\cos\theta)^2} \text{ .}$$

Therefore, the total surface settlement induced by excavating the infinitesimal thin slice is the summation of the settlement component (S_{ABCD}) due to changes of forces acting on the curve surface *ABCD* and the component settlement (S_{CX}) caused by changes of forces acting on the two end sections CX_1 and CX_2. The settlement components, S_{ABCD}, and S_{CX}, can be obtained by integrating and summation of the contribution from $\delta_{dP}, \delta_{dQ}, \delta_{dT_1}$ and δ_{dT_2} as follows:

$$S_{ABCD} = \left(\int_{\theta_1}^{\theta_2} (\delta_{dP}\,\mathrm{d}\theta + \int_{\theta_1}^{\theta_2} \delta_{dQ}\mathrm{d}\theta\right)\mathrm{d}v \text{ ,} \qquad (5a)$$

$$S_{CX} = S_{CX1} + S_{CX2} = \int_{\theta_1}^{\theta_2}\int_0^{r_0} \delta_{dT_1}\mathrm{d}\theta\mathrm{d}r + \int_{\theta_1}^{\theta_2}\int_0^{r_0} \delta_{dT_2}\mathrm{d}\theta\mathrm{d}r \text{ . (5b)}$$

Obviously, for a circular tunnel with radius r_o, the limiting angle θ lies between $\theta_1 = 0$ and $\theta_2 = 2\pi$ and the radial distance r goes from 0 to r_0.

1.4 Total surface settlement due to the excavation of entire tunnel

Now it is appropriate to consider the total surface settlement at any surface point $(x, y, 0)$. If S_1 is the total surface settlement due to the changes of forces acting on the entire curved surface *CF* along the length of the tunnel, i.e., $L = v_2 - v_1$, it is in fact contributed by each infinitesimal thin slice *ABCD* (see Figure 2). Thus, by making use of Equation 5(a), S_1 can be obtained by integration and written as follows:

$$S_1 = \int_{v_1}^{v_2} S_{ABCD}\mathrm{d}v = \int_{v_1}^{v_2}\int_{\theta_1}^{\theta_2} \delta_{dP}\mathrm{d}\theta\mathrm{d}v + \int_{v_1}^{v_2}\int_{\theta_1}^{\theta_2} \delta_{dQ}\mathrm{d}\theta\mathrm{d}v$$
$$= k\frac{(1-\mu)\rho h r_0}{2\pi G} I_1 + k\frac{\rho h r_0}{4\pi G} I_2 +$$
$$kk_0 \frac{\rho h r_0}{4\pi G} I_3 - kk_0 \frac{\rho(1-2\mu)hr_0}{4\pi G} I_4 \text{ ,} \qquad (6)$$

where $I_i = \int_{v_1}^{v_2}\int_{\theta_1}^{\theta_2} f_i(\theta, v)\mathrm{d}\theta\mathrm{d}v$ $(i = 1 \sim 4)$,

$$f_1(\theta, v) = \frac{\cos\theta}{R_{CF}} \text{ , } f_2(\theta, v) = \frac{\cos\theta(h-r_0\cos\theta)^2}{R_{CF}^3} \text{ ,}$$
$$f_3(\theta, v) = \frac{\sin\theta(x-r_0\sin\theta)(h-r_0\cos\theta)}{R_{CF}^3} \text{ ,}$$
$$f_4(\theta, v) = \frac{\sin\theta(x-r_0\sin\theta)}{R_{CF}(R_{CF}+h-r_0\cos\theta)} \text{ .}$$

The cumulative effects of all internal $\mathrm{d}T_1$ and $\mathrm{d}T_2$ acting on each internal infinitesimal slice on the total surface settlement are cancelled out each other, except the two forces acting on the end faces, EF_1 and EF_2, of the tunnel. Thus, if S_2 is the total surface settlement induced ($S_{EF1} + S_{EF2}$) by the boundary forces $\mathrm{d}T_1$ and $\mathrm{d}T_2$, then by considering the expression given in Equation5 (b), S_2 can be simply written as follows:

$$S_2 = S_{EF1} + S_{EF2} = \int_{\theta_1}^{\theta_2}\int_0^{r_0} \delta_{dT_1}\mathrm{d}\theta\mathrm{d}r + \int_{\theta_1}^{\theta_2}\int_0^{r_0} \delta_{dT_2}\mathrm{d}\theta\mathrm{d}r$$
$$= -kk_0 \frac{\rho h(y-v_1)}{4\pi G} I_5 + kk_0 \frac{(1-2\mu)\rho h(y-v_1)}{4\pi G} I_6 +$$
$$kk_0 \frac{\rho h(y-v_2)}{4\pi G} I_7 - kk_0 \frac{(1-2\mu)\rho h(y-v_2)}{4\pi G} I_8 \text{ ,} \qquad (7)$$

where

$$I_i = \int_{\theta_1}^{\theta_2}\int_0^{r_0} f_i(r, \theta)\mathrm{d}r\mathrm{d}\theta \text{ } (i = 5 \sim 8),$$
$$f_5(r, \theta) = \frac{r(h-r\cos\theta)}{R_{EF}^3} \text{ ,}$$
$$f_6(r, \theta) = \frac{r}{R_{EF}(R_{EF}+h-r\cos\theta)} \text{ ,}$$
$$R_{EF} = \sqrt{(x-r\sin\theta)^2+(y-v_1)^2+(h-r\cos\theta)^2} \text{ ,}$$

$f_7(r, \theta)$ and $f_8(r, \theta)$ have the similar expressions to $f_5(r, \theta)$ and $f_6(r, \theta)$, respectively, they can be obtained by replacing v_1 with v_2 in the expression of R_{EF}.

For simplicity, $f_1(\theta, v)$ to $f_8(r, \theta)$ are firstly approximated with polynomials using the Taylor's series expansion. The integrals of I_1 to I_6 are then carried out, the expressions are shown in Appendix. I_7 and I_8 have the similar expressions with I_5 and I_6 respectively, just replaces v_1 with v_2.

The total surface displacement is the summation of S_1 and S_2 as follows:

$$S = S_1 + S_2 = k\frac{(1-\mu)\rho h r_0}{2\pi G} I_1 + k\frac{\rho h r_0}{4\pi G} I_2 +$$

$$kk_0\frac{\rho hr_0}{4\pi G}I_3-kk_0\frac{(1-2\mu)\rho hr_0}{4\pi G}I_4-kk_0\frac{\rho h(y-v_1)}{4\pi G}I_5+$$
$$kk_0\frac{(1-2\mu)\rho h(y-v_1)}{4\pi G}I_6+kk_0\frac{\rho h(y-v_2)}{4\pi G}I_7-$$
$$kk_0\frac{(1-2\mu)\rho h(y-v_2)}{4\pi G}I_8\ . \tag{8}$$

The above equations are programmed in Mathematica 4.0[8] to calculate surface ground settlement and to draw two or three-dimensional settlement profiles.

2 Verifications of the approximate solution

2.1 Three-dimensional numerical finite element (FE) analysis

In order to verify the approximate analytical solution, the finite element method (FEM) is used to model a tunnel constructed in an elastic soil three-dimensionally. The finite element mesh generated by a commercially available computer software – ABAQUS (Hibbitt, Karlsson & Sorensen Inc (1998)[9] is shown in Figure 5(a). Only one half of the tunnel and the ground are analyzed as a plane of symmetry is identified at x=0. The finite element mesh is 124 m long, 54 m high and 162.5 m wide, the boundaries of the mesh are enough far away from the tunnel for eliminating the influences of boundary restraints.

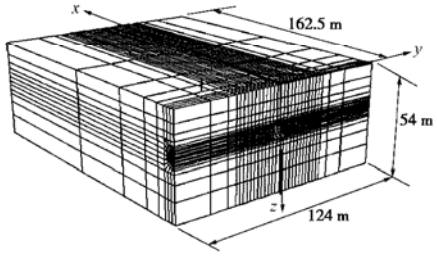

(a) Isotropic view

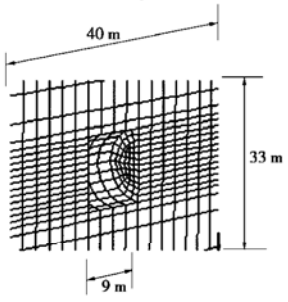

(b) Close-up view of tunnel zone

Fig. 5 Finite element mesh

The mesh consists of 5040 elements and 5642 nodes. Eight-node elastic brick elements are used to model the soil. Roller supports are applied on all vertical sides of the mesh while pin supports are assigned to the base of the mesh. Therefore, the movements in the normal direction to all vertical sides of the mesh and the movements in all directions at the base of the mesh are restrained. The tunnel diameter, D, is 9 m; the cover depth to the crown of the tunnel, C, is 18 m.

Table 1 summarizes the parameters used in the three-dimensional FE analysis. During the FE analysis, a segment of the tunnel, L=9 m, is excavated as shown in Figure 5(b). No supporting pressures and no lining is applied during excavation, the stress relief coefficient used in the analytical solution is 1.0.

Table 1 Summary of parameters

Parameters	Magnitude
Tunnel diameter, D/m	9 (r_0=4.5 m)
Cover depth above tunnel, C /m	18(h=22.5 m)
Unit weight, r/(kN • m^{-3})	15
Shear modulus of soil, G/MPa	7.69
Possion's ratio of soil, μ	0.30
Earth pressure coefficient at rest, k_0	0.49
Tunnel excavation length, L/m	9

2.2 Comparison between numerical FE analysis and analytical approximation

Figure 6 compares the settlement profiles obtained by the numerical FE analysis and the analytical approximations at the middle section of the tunnel. It can be seen that the shape and the width of the settlement troughs computed by the two methods using k_0=0.49 are very consistent, with only small difference in the maximum settlement, S_{max}, at the centre of the settlement troughs. The computed S_{max} are 6.4 mm and 7.0 mm by the analytical method and FEM respectively, equivalent to an 8.6% error if the FEM can be regarded as error free. This magnitude of error is likely to be acceptable for most of preliminary engineering design calculations.

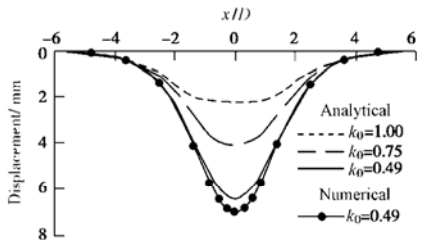

Fig. 6 Transverse settlement profile due to excavation of a single tunnel

In order to demonstrate the usefulness of the analytical solution, ground settlements are also

calculated using different k_0 values (i.e., 0.75 and 1.0). As expected, the depth of the calculated settlement trough increases as the k_0 value decreases.

3 Applications of the solution

3.1 Settlements due to excavation of two parallel tunnels

Figure 7 shows two parallel circular tunnels. The two tunnels are 4.5 m in radius (or D=D_1=D_2=9 m in diameter) and separated at 18 m (i.e., 2D) from the centre-line to the centre-line (c/c) of the two tunnels. The cover depth ($C_1=C_2$) is 18 m from the ground surface and the excavation length L is 36 m (i.e, $L=L_1=L_2=4D$). The elastic soil is assumed to have a density of $\rho=18$ kN/m^3 with an initial earth pressure at rest, $k_0=0.49$. The elastic parameters of the soil are assumed to be $G=3.85$ MPa and $\mu=0.3$. To illustrate the capability of modelling supporting pressure used in tunnels, the stress relief coefficient, k, is set to be 0.5, which can be regarded as supporting pressure equal to 50% of the initial earth pressure is applied inside the tunnels to maintain face stability during excavation.

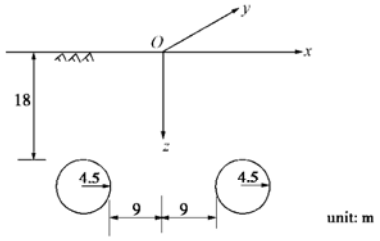

Fig. 7 Cross-section of two parallel tunnels

Figure 8 shows the calculated three-dimensional settlement profile and the transverse settlements due to the construction of the two tunnels. The contribution of each tunnel to the total settlement is illustrated in the figures. The resulting settlement trough is the superposition of two settlement troughs due to the excavation of a single tunnel. The maximum settlement is 20.5 mm located on either side of the centreline of the two tunnels.

3.2 Settlements due to excavation of two cross tunnels

Figure 9 illustrates the dimensions and the orientation of two cross tunnels. The two tunnels have the same diameter D=D_1=D_2=9 m. The lower (or deeper) tunnel has a cover depth C_1=4D and an excavation length L_1=100 m; whereas the upper tunnel has a cover depth C_2=2D with an excavation length L_2=50 m. The values of k_0, k, and soil parameters are the same with the case of above parallel tunnels.

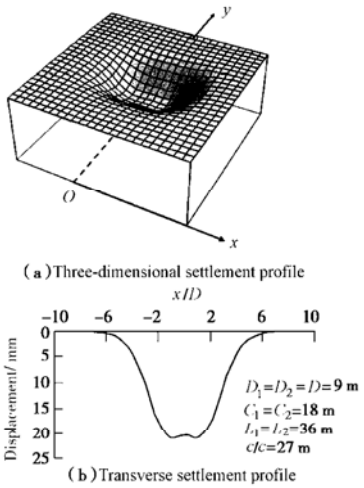

Fig. 8 Settlement profile due to excavation of two parallel tunnels

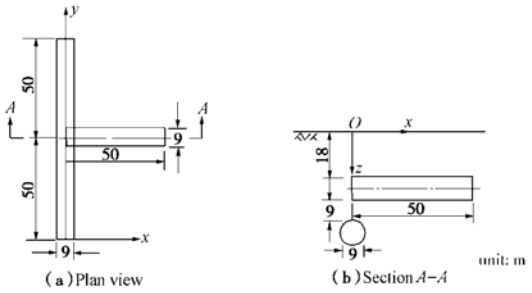

Fig. 9 Dimensions of two cross tunnels

Figure 10 depicts the three-dimensional settlement profile and transverse settlements along the longitudinal centre-line of the upper tunnel. As expected, an unsymmetrical settlement profile about the x-axis but symmetric about the y-axis can be clearly seen in both figures. The transverse settlement trough does not follow the Gaussian distribution because of the unsymmetrical orientation of two tunnels. The maximum calculated settlement is 19.2 mm.

4 Summary and conclusions

An approximate explicit analytical solution, based on the integrated form of Mindlin's equations and Taylor's series expansions, has been derived to calculate two- and three-dimensional surface settlements due to the excavation of either single or multiple tunnels in a homogeneous elastic soil with an arbitrary orientation during tunnel advancement in less than a few seconds. An arbitrary supporting pressure can be modelled inside

the tunnel by using a stress relief coefficient. The derived analytical solution has been verified by carrying out a three-dimensional finite element analysis of a single tunnel excavation. It was found that the discrepancy between the simplified approximate solution and the finite element analysis was less than 9%, which is considered to be accurate enough for many preliminary engineering analyses and designs. The usefulness of the simplified approximate solution has been demonstrated by analyzing twin parallel and two cross tunnels.

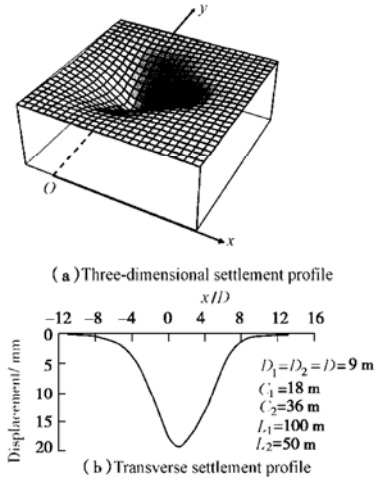

Fig. 10 Settlement profile due to excavation of two cross tunnels

It should be noted that, for soft rock or soft soil ground, the analytical solution may contain considerable error because of its elastic supposition. But at low extent of stress relief (i.e., good supporting procedure in tunnelling in most cases), the analytical solution is still available.

Acknowledgements

This research project is supported by research grant CRC96/99.EG04 from the Research Grants Council of HKSAR. The authors would like to acknowledge the assistance provided by Mr Gordon Lee for carrying out the finite element analysis reported in this paper.

References:

[1] PECK R B. Deep excavations and tunneling in soft ground[C]// Proc 7th International Conference on Soil Mechanics and Foundation Engineering, Mexico City, State of the Art Volume, 1969: 266 – 290.

[2] O'REILLY M P, NEW B M. Settlement above tunnels in the United Kingdom-their magnitude and prediction[C]// Tunnelling'82, London IMM, 1982: 173 – 181.

[3] ATTEWELL P B, WOODMAN J P. Predicting the dynamics of ground settlement and its derivates by tunneling in soil[J]. Ground Engrg, 1982, **15**: 13 – 22.

[4] SAGASETA C. Analysis of undrained soil deformation due to ground loss[J]. Geotechnique, 1987, **37**: 301 – 320.

[5] VERRUIJT A, BOOKER J R. Surface settlements due to the formation of a tunnel in an elastic half plane[J]. Geotechnique, 1996, **46**(4): 753 – 756.

[6] MINDLIN R D. Force at a point in the interior of a semi-infinite solid[J]. J Appl Phys, 1936, **7**(5): 195 – 202.

[7] VAZIRI H, SIMPSON B, PAPPIN J W, SIMPSON L. Integrated forms of Mindlin's equations[J]. Geotechnique, 1982, **32**(3): 275 – 278.

[8] Wolfram Research Inc. Mathematica[CP]. Version number 4.0100 Trade Center Drive Champaign, IL 61820, USA, 1998.

[9] HIBBITT Karlsson, Sorensen Inc. ABAQUS User's manual[CP]. Version 5.8. 1998.

Appendix:

With the help of Mathmatica 4.0 (1988), Expressions of $I_1 \sim I_6$ in equations become

$$I_1 = \left[\left\{ A_1\theta + A_2 \sin\theta + A_3 \sin 2\theta + A_4 \sin 3\theta \right\}_{\theta=\theta_1}^{\theta=\theta_2} \right]_{v=v_1}^{v=v_2},$$

$$I_2 = \left[\left\{ B_1\theta + B_2 \sin\theta + B_3 \sin 2\theta + B_4 \sin 3\theta \right\}_{\theta=\theta_1}^{\theta=\theta_2} \right]_{v=v_1}^{v=v_2},$$

$$I_3 = \left[\left\{ C_1\theta + C_2 \cos\theta + C_3 \sin 2\theta \right\}_{\theta=\theta_1}^{\theta=\theta_2} \right]_{v=v_1}^{v=v_2},$$

$$I_4 = \left[\left\{ D_1\theta + D_2 \cos\theta + D_3 \sin 2\theta \right\}_{\theta=\theta_1}^{\theta=\theta_2} \right]_{v=v_1}^{v=v_2},$$

$$I_5 = \left[\left\{ E_1\theta + E_2 \sin\theta + E_3 \sin 2\theta \right\}_{\theta=\theta_1}^{\theta=\theta_2} \right]_{r=0}^{r=r_0},$$

$$I_6 = \left[\left\{ F_1\theta + F_2 \sin\theta + F_3 \sin 2\theta \right\}_{\theta=\theta_1}^{\theta=\theta_2} \right]_{r=0}^{r=r_0},$$

Where

$$A_1 = -\frac{r_0 h(y-v)}{2R_{CF1}^2 R_{CF0}},$$

$$A_2 = \ln(R_{CF0} - y + v) - \frac{3r_0^2(y-v)(h^2 + R_{CF0}^2)}{8R_{CF1}^2 R_{CF0}^3},$$

$$A_3 = -\frac{r_0 h(y-v)}{4R_{CF1}^2 R_{CF0}},$$

$$A_4 = -\frac{r_0^2(y-v)(h^2 - R_{CF0}^2)}{24R_{CF1}^2 R_{CF0}^3},$$

$$B_1 = -\frac{h^3 r_0 (y-v)}{2R_{CF1}^2 R_{CF0}^3} + \frac{hr(r_0 - x)^2 (y-v)}{R_{CF1}^4 R_{CF0}},$$

$$B_2=-\frac{9h^4r_0^2(y-v)}{8R_{CF1}^2R_{CF0}^5}+\frac{3h^2r_0^2(y-v)(5R_{CF1}^2-4h^2)}{8R_{CF1}^4R_{CF0}^3}-$$
$$\frac{(y-v)(4h^6+8h^4(r_0-x)^2+3r^2(r_0-x)^4-h^2(5r_0-2x)(r_0-x)^2(r_0+2x))}{4R_{CF1}^6R_{CF0}},$$

$$B_3=\frac{hr_0(r_0-x)^2(y-v)}{2R_{CF1}^4R_{CF0}}-\frac{h^3r_0(y-v)}{4R_{CF1}^2R_{CF0}^3},$$

$$B_4=-\frac{h^4r_0^2(y-v)}{8R_{CF1}^2R_{CF0}^5}+\frac{h^2r_0^2(y-v)(5R_{CF1}^2-4h^2)}{24R_{CF1}^4R_{CF0}^3}-$$
$$\frac{r_0^2(r_0-x)^2(y-v)(R_{CF1}^2-4h^2)}{12R_{CF1}^6R_{CF0}},$$

$$C_1=\frac{9r_0^2h(r_0-x)^3(y-v)}{4R_{CF1}^2R_{CF0}^5}+$$
$$\frac{r_0h(r_0-x)(y-v)(-22h^2r_0+2r_0^3+4h^2x-6r_0x^2+4x^3)}{8R_{CF1}^4R_{CF0}^3}+$$
$$\frac{r_0h(y-v)(h^4-9h^2r_0(r_0-x)+(r_0-x)^3(2r_0+x))}{2R_{CF1}^6R_{CF0}},$$

$$C_2=\frac{3r_0^2h(r_0-x)^3(y-v)}{R_{CF1}^2R_{CF0}^5}+$$
$$\frac{r_0h(r_0-x)(y-v)(-4h^2r_0+h^2x+r_0^2x-2r_0x^2+x^3)}{R_{CF1}^4R_{CF0}}+$$
$$\frac{h(y-v)(h^4x+x(r_0-x)^3(3r_0-x)-2h^2(r_0-x)(4r_0^2-2r_0x+x^2))}{R_{CF1}^6R_{CF0}},$$

$$C_3=\frac{-3r_0^2h(r_0-x)^3(y-v)}{8R_{CF1}^2R_{CF0}^5}+$$
$$\frac{r_0h(r_0-x)(y-v)(5h^2r_0+r_0^3-2h^2x-4r_0^2x+5r_0x^2-2x^3)}{8R_{CF1}^4R_{CF0}^3}-$$
$$\frac{r_0h(y-v)(h^4-3h^2r_0(r_0-x)+(r_0-x)^3x)}{4R_{CF1}^6R_{CF0}},$$

$$D_1=\arctan\left(\frac{h(y-v)}{(r_0-x)R_{CF0}}\right)-\arctan\left(\frac{h(y-v)(h+R_{CF0})}{(r_0-x)(R_{CF0}^2+hR_{CF0})}\right)-$$
$$\frac{hr_0(R_{CF0}^2+(r_0-x)^2)(y-v)}{R_{CF1}^2(R_{CF0}^2-h^2)R_{CF0}}-\frac{3r_0^2R_{CF0}(r_0-x)(y-v)}{2h(R_{CF0}^2-h^2)^2}+$$
$$\frac{3r_0R_{CF0}(2h^2+r_0^2-r_0x)(y-v)}{4h^3(R_{CF0}^2-h^2)}+\frac{3r_0^2(r_0-x)^3(y-v)}{4hR_{CF1}^2R_{CF0}^3}-$$
$$\frac{3r_0(r_0-x)(y-v)(h^4(5r_0-2x)+r_0(r_0-x)^4+2h^2(r_0-x)^2(2r_0-x))}{4h^3R_{CF1}^4R_{CF0}}+$$
$$\frac{3r_0^2(r_0-x)(y-v)}{2(R_{CF0}^2-h^2)^2}-\frac{r_0(y-v)}{2(R_{CF0}^2-h^2)},$$

$$D_2=-\arctan\left(\frac{y-v}{r_0-x}\right)+\arctan\left(\frac{h(y-v)}{(r_0-x)R_{CF0}}\right)-$$
$$\frac{r_0(y-v)}{(R_{CF0}^2-h^2)}-\frac{hr_0(R_{CF0}^2+(r_0-x)^2)(y-v)}{R_{CF1}^2(R_{CF0}^2-h^2)R_{CF0}}-$$
$$\frac{2r_0^2R_{CF0}(r_0-x)(y-v)}{h(R_{CF0}^2-h^2)^2}+\frac{r_0R_{CF0}(2h^2+r_0^2-r_0x)(y-v)}{h^3(R_{CF0}^2-h^2)}+$$
$$\frac{r_0^2(r_0-x)^3(y-v)}{hR_{CF1}^2R_{CF0}^3}-$$
$$\frac{r_0(r_0-x)(y-v)(h^4(5r_0-2x)+r_0(r_0-x)^4+2h^2(r_0-x)^2(2r_0-x))}{h^3R_{CF1}^4R_{CF0}}+$$
$$\frac{2r_0^2(r_0-x)(y-v)}{(R_{CF0}^2-h^2)^2},$$

$$E_1=-\frac{3h^3r^3(y-v_1)}{4R_{EF1}^2R_{EF0}^5}-\frac{hr^3(y-v_1)(h^2-3(r-x)^2)}{4R_{EF0}^4R_{EF1}^3}-$$
$$\frac{rh(y-v_1)(2h^4-(r-x)^2(r^2+4rx-2x^2)+h^2(5r^2-8rx+4x^2))}{2R_{EF1}^6R_{EF0}},$$

$$E_2=-\frac{r^2h^2(y-v_1)}{R_{EF1}^2R_{EF0}^3}+\frac{r^2(y-v_1)((r-x)^4-h^4)}{R_{EF1}^6R_{EF0}},$$

$$E_3=-\frac{3r^3h^3(y-v_1)}{8R_{EF1}^2R_{EF0}^5}-\frac{r^3h(y-v_1)(h^2-3(r-x)^2)}{8R_{EF1}^4R_{EF0}^3}-$$
$$\frac{r^3h(y-v_1)(4h^2-3R_{EF1}^2)}{4R_{EF1}^6R_{EF0}},$$

$$F_1=\frac{x}{y-v_1}\arctan\left(\frac{r-x}{y-v_1}\right)+$$
$$\lg\left(\frac{4R_{EF3}(R_{EF0}+h)\sqrt{(y-v_1)^2}}{h^2R_{EF2}}\right)-\frac{x}{y-v_1}\beta-$$
$$\frac{(2h^5+h^3(3r^2-4rx+4R_{EF2}^2)-4rhxR_{EF2}^2+}{4R_{EF3}^4}\rightarrow$$
$$\leftarrow\frac{2hR_{EF2}^4+r^2h(2x^2+3(y-v_1)^2))(R_{EF0}^2-r^2+rx)}{R_{EF0}^3},$$

where β is given by

$$\begin{cases}\beta=\arctan[\alpha] & (\alpha_1\geq 0),\\ \beta=\pi+\arctan[\alpha] & (\alpha_1\leq 0 \text{ but } \alpha_2\geq 0),\\ \beta=-\pi+\arctan[\alpha] & (\alpha_1\leq 0 \text{ and } \alpha_2\leq 0),\end{cases}$$

$$\alpha_1=(h^2+hR_{EF0})(2x-r)+xR_{EF4}^2,$$

$$\alpha_2=((h^2+hR_{EF0})((r-x)x+(y-v_1)^2)+R_{EF4}^2(y-v_1)^2)(y-v_1),$$

$$\alpha=\frac{((r-x)x+(y-v)^2)(h^2+hR_{EF0})+R_{EF4}^2(y-v)^2}{((v-y)(xR_{EF4}^2-(r-2x)(h^2+hR_{EF0}))},$$

$$F_2=-\frac{(h^2(r+x)+xR_{EF2}^2+r(v_1-x-y)(v_1+x-y))}{R_{EF3}^2R_{EF0}}+$$
$$\ln(r-x+R_{EF0}),$$

$$F_3=-\frac{2h^5+h^3(3r^2-4rx+4R_{EF2}^2)-4rhxR_{EF2}^2+}{8R_{EF3}^4}\rightarrow$$
$$\leftarrow\frac{2hR_{EF2}^4+r^2h(2x^2+3(y-v_1)^2)}{R_{EF0}},$$

$$R_{CF1}=\sqrt{h^2+(x-r_0)^2},$$

$$R_{EF1}=\sqrt{h^2+(x-r)^2},$$

$$R_{EF2}=\sqrt{x^2+(y-v_1)^2},$$

$$R_{EF3}=\sqrt{h^2+(y-v_1)^2},$$

$$R_{EF4}=\sqrt{(r-x)^2+(y-v_1)^2}.$$